Electronic Supplementary Material (ESI) for Journal of Materials Chemistry A.

Supporting Information

Tuning Charge Transfer Route by P-N Junction Catalysts Embedded with CdS Nanorods for Simultaneously Efficient Hydrogen and Oxygen Evolution

*Kan Zhang, Wanjung Kim, Ming Ma, Xinjian Shi, Jong Hyeok Park**

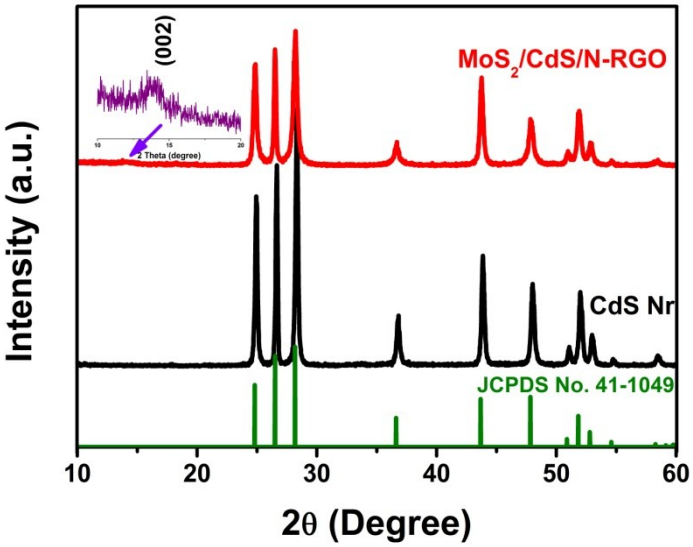

Figure S1. XRD patterns of CdS Nrs and MoS_2/CdS/N-RGO hybrid.

The XRD patterns of the CdS Nrs and MoS_2/CdS/N-RGO hybrid have shown that the diffraction peaks match the standard peaks of hexagonal CdS with lattice constants of α = 0.414 nm and c = 0.673 nm (JCPDS card No. 41-1049). Magnification of the XRD pattern of MoS_2/CdS/N-RGO hybrid showed a diffraction hump at 14.2°, corresponding to the (002) MoS_2 plane.

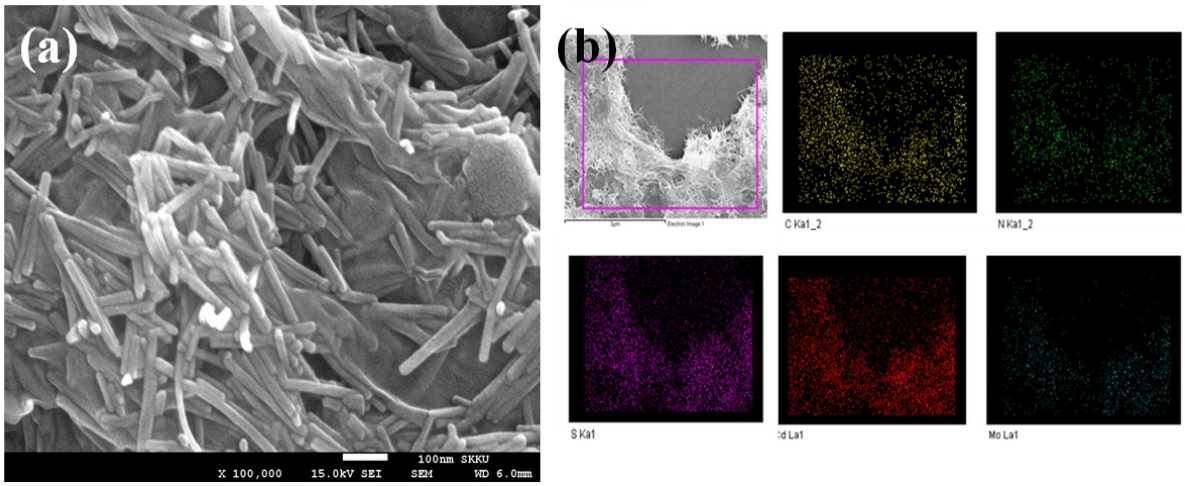

Figure S2. SEM image of the MoS_2/CdS/N-RGO hybrid (a) andelement mapping of the MoS_2/CdS/N-RGO hybrid (b).

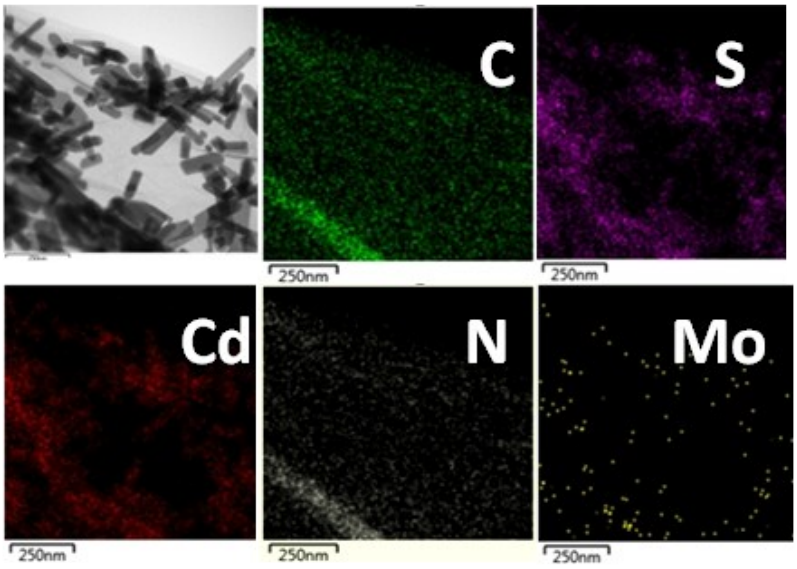

Figure S3. Element mapping of the MoS_2/CdS/N-RGO hybrid in high resolution.

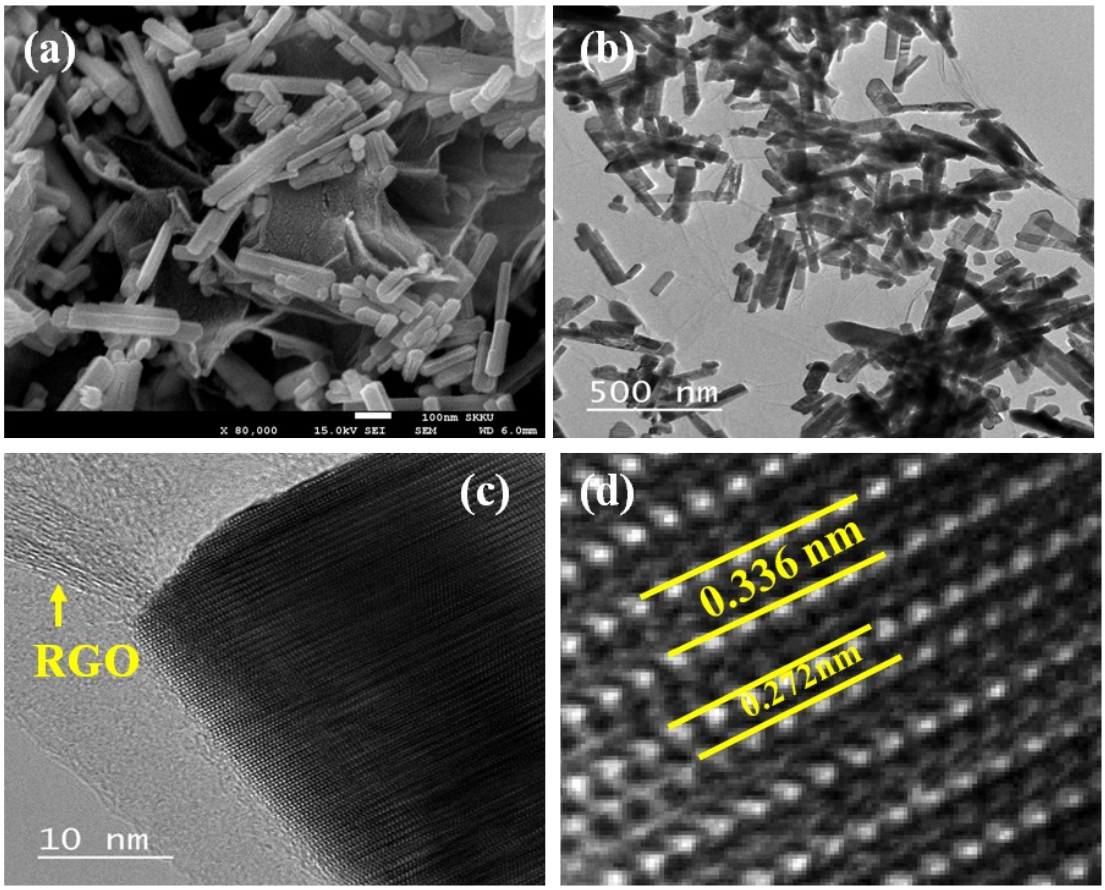

Figure S4. TEM and HR-TEM images of the type I MoS_2/N-RGO/CdS hybrid.

The SEM and TEM imgaes of type I MoS_2/N-RGO/CdS hybrid show the topical morphology and it is noteworthy that the atom arrangement of CdS exhibits different lattice spacing, suggesting high degree of defect in CdS Nr.

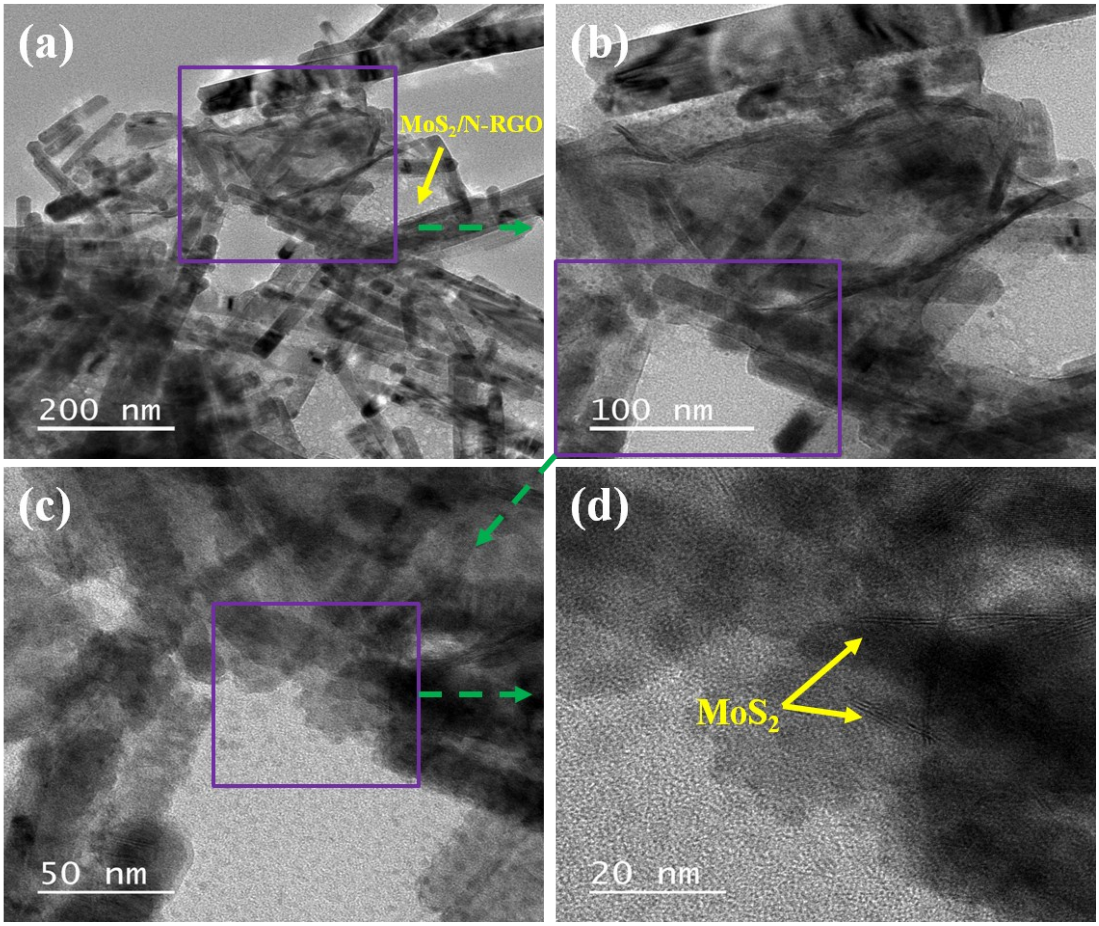

Figure S5. TEM and HR-TEM images of the type II MoS_2/N-RGO/CdS hybrid.

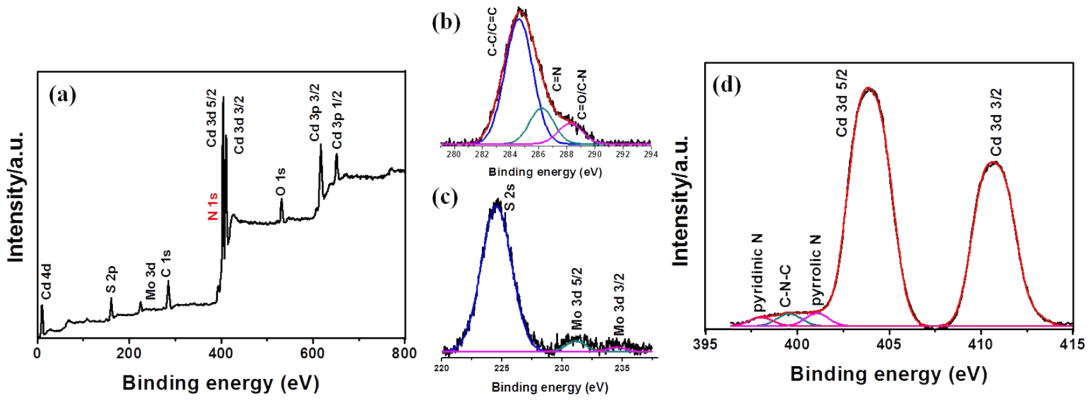

Figure S6. XPS spectrum of the MoS_2/CdS/N-RGO hybrid, (b) High-resolution C1s XPS spectrum of the MoS_2/CdS/N-RGO hybrid, (c) High-resolution S2p and Mo3d XPS spectrum of the MoS_2/CdS/N-RGO hybrid, (d) High-resolution N1s and Cd3d XPS spectrum of the MoS_2/CdS/N-RGO hybrid.

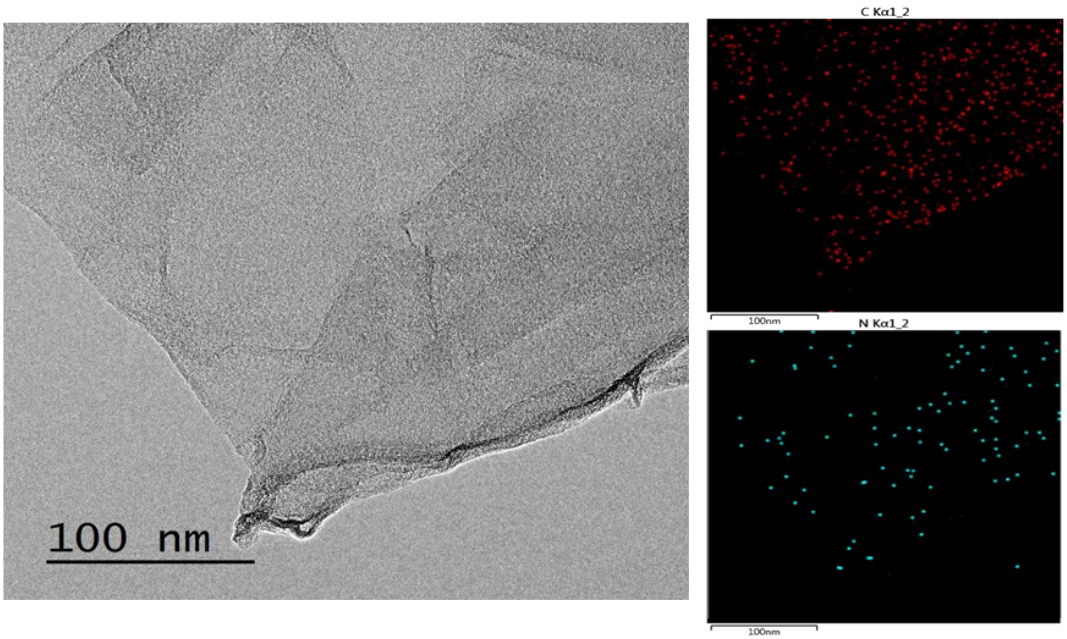

Figure S7. TEM and STEM images of the N-RGO sheet.

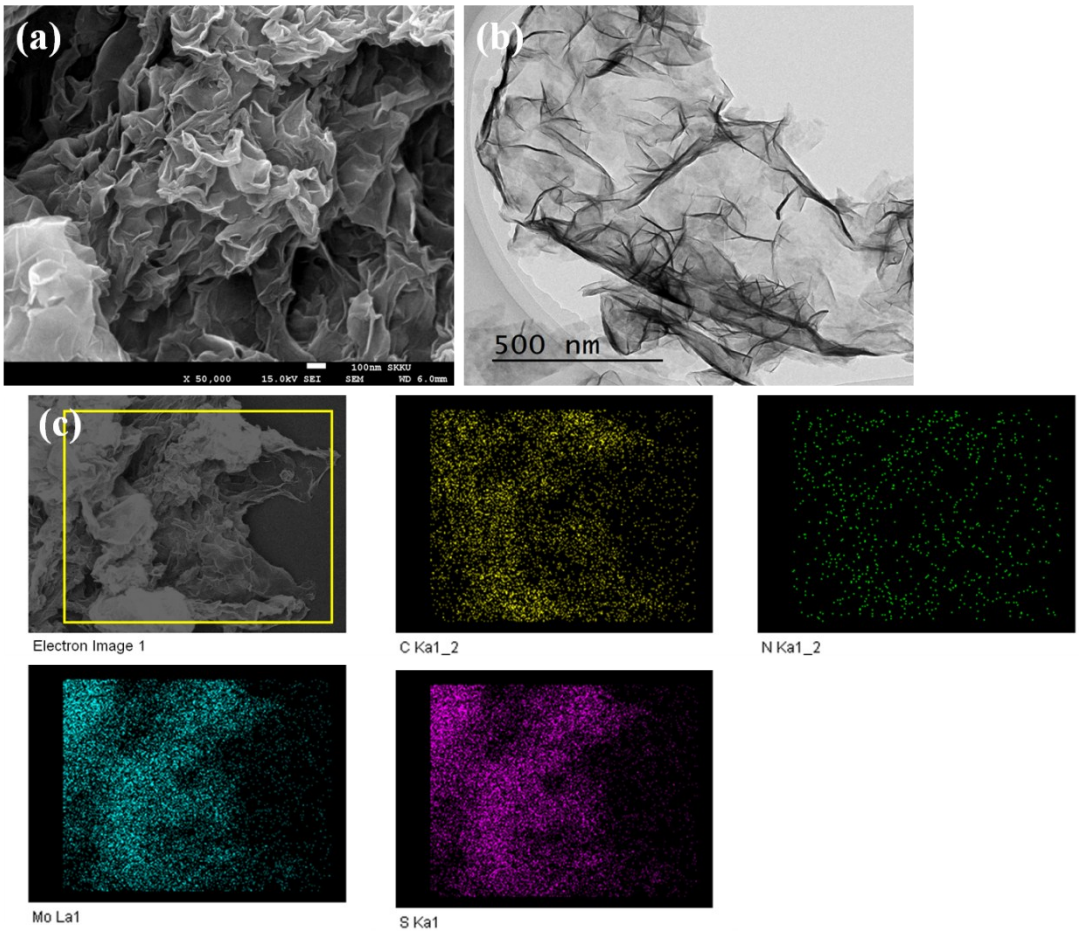

Figure S8. SEM, TEM images and element mapping of the MoS_2/N-RGO hybrid.

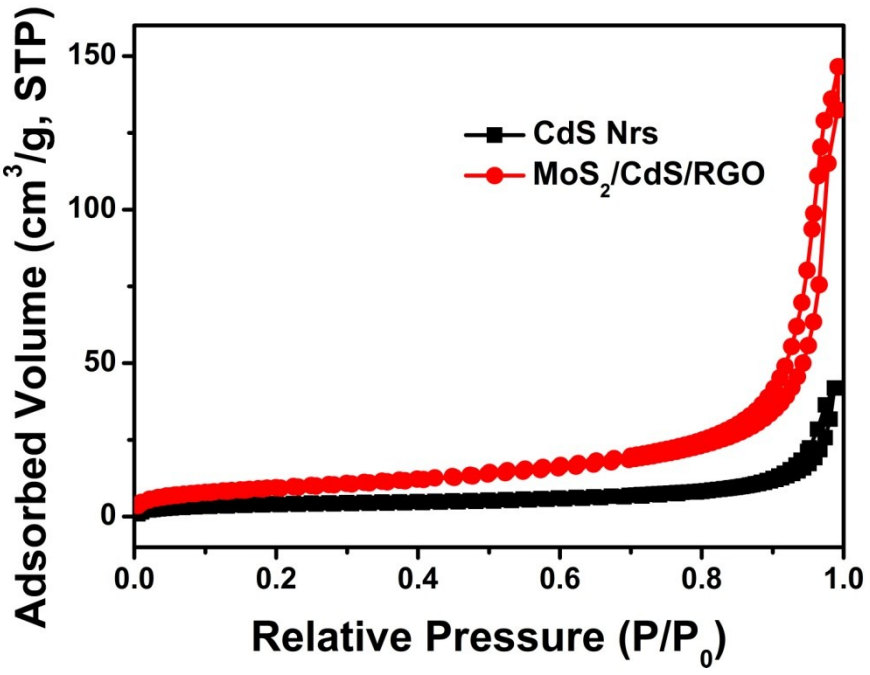

Figure S9. The adsorption-desorption isotherms of pure CdS Nrs and MoS_2/CdS/RGO hybrid.

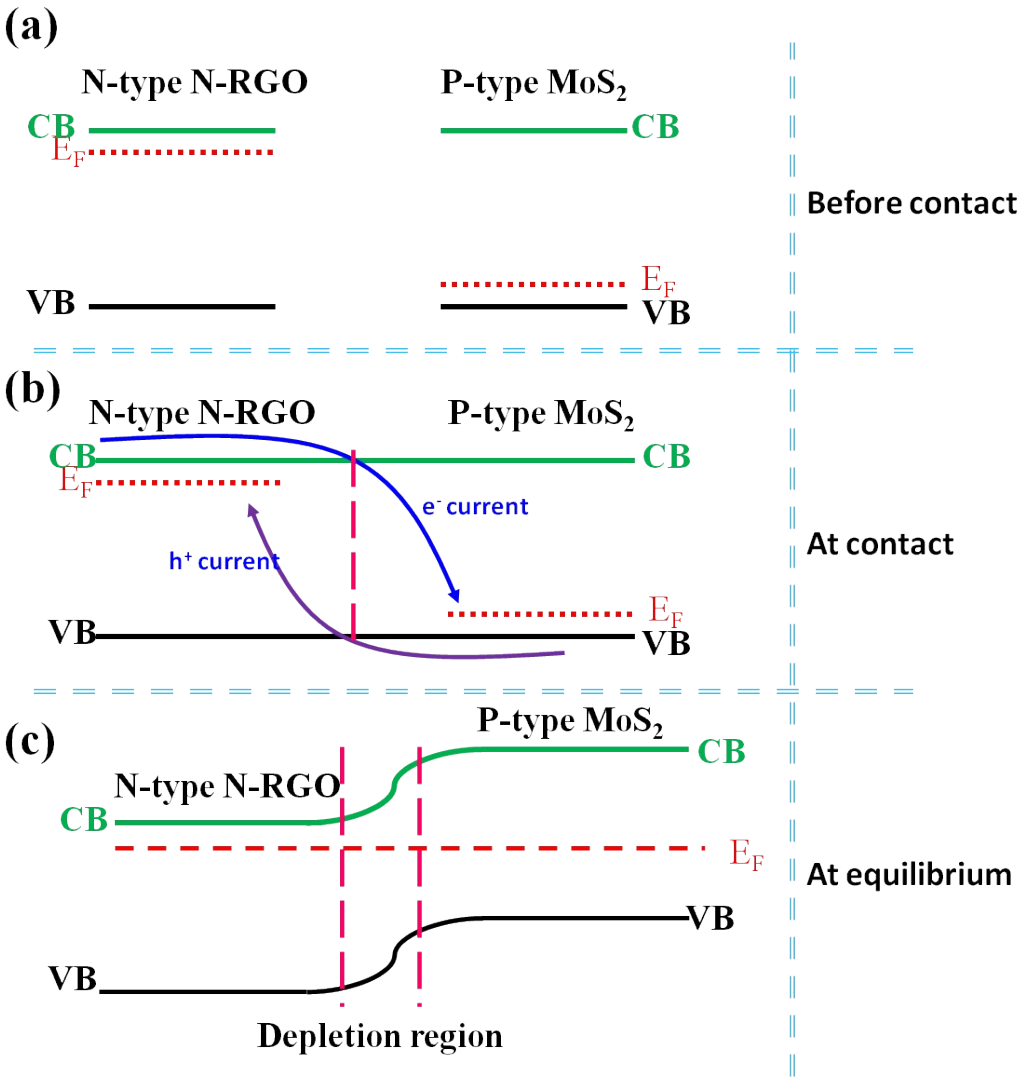

Figure S10. Potential variation of MoS_2/N-RGO during p/n junction formation process.

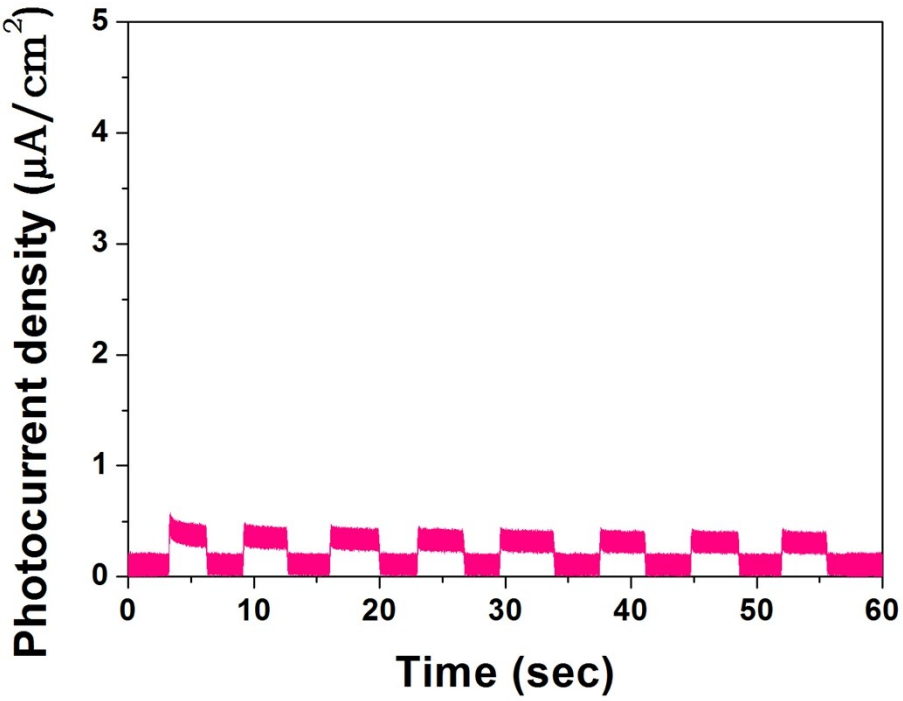

Figure S11. The transient photocurrent responses of MoS_2/N-RGO hybrid electrodes at 0.6 V vs Ag/AgCl in 1M NaOH aqueous solution under solar light irradiation. Notes that pure MoS_2 and N-RGO electrodes didn't show photoresponse properties.

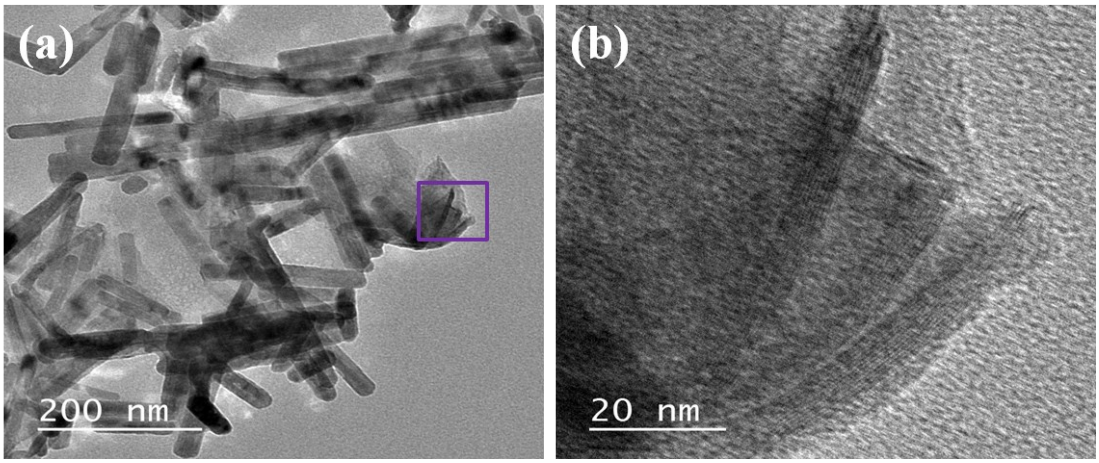

Figure S12. TEM images of the MoS_2/CdS hybrid.

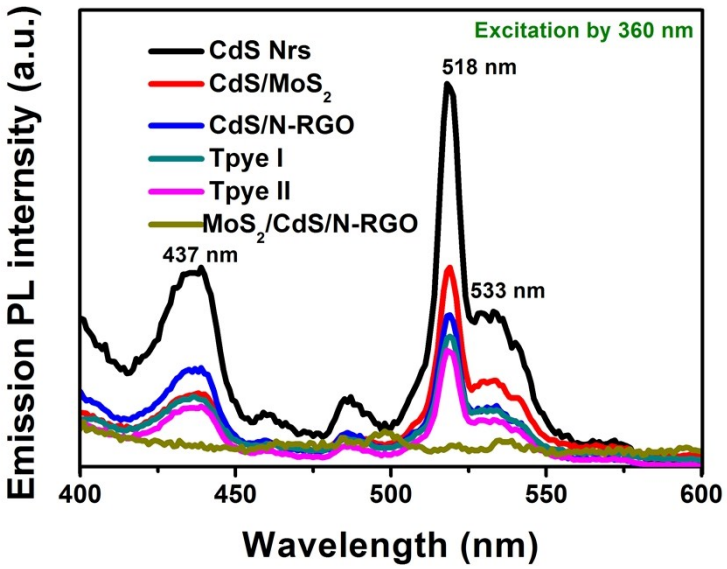

Figure S13. Photoluminescence (PL) spectra of CdS Nrs, MoS_2/CdS, MoS_2/N-RGO, type I MoS_2/N-RGO/CdS, type II MoS_2/N-RGO/CdS and MoS_2/CdS/N-RGO hybrid with an excitation wavelength of 360 nm.

The CdS also has a strong emission at 518 nm which extends to 550 nm. This peak is attributed to the band-band PL phenomenon with the energy of light approximately equal to their band-gap energy. And a broad emission at 437 nm corresponds to the extrinsic deep-level emission.

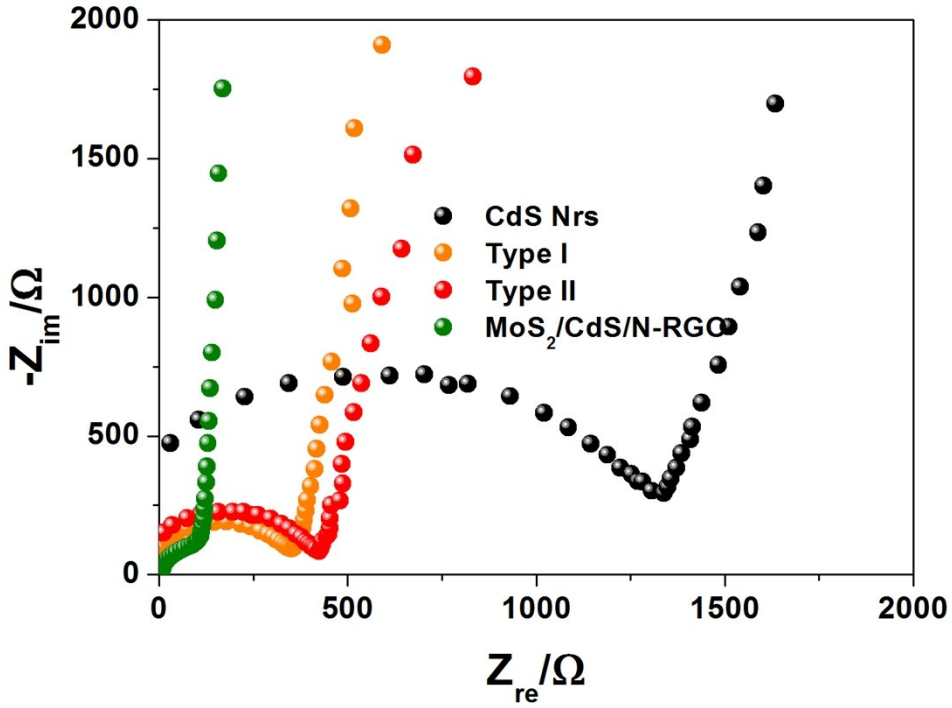

Figure S14. EIS changes of CdS Nrs, type I MoS_2/N-RGO/CdS, type II MoS_2/N-RGO/CdS and MoS_2/CdS/N-RGO hybrid. The EIS measurements were performed in the presence of a 1 mM $K_3[Fe(CN)_6]/K_4[Fe(CN)_6]$ (1:1) mixture as a redox probe in 0.5 M KCl aqueous solution.